STScI | SPACE TELESCOPE SCIENCE INSTITUTE

Instrument Science Report ACS 2017-04

Updated Measurements of ACS/SBC Dark Rates

R.J. Avila

May 3, 2017

Abstract

The results of dark rate monitoring programs for the ACS/SBC are presented here. The dark rate has a very low and stable value of 8.11×10^{-6} *cts/pix/s when the instrument is* $\lesssim 25.^{\circ}C$*. In a 1000s exposure, less than 1% of pixels will have 1 count. As the instrument warms up, the overall dark rate increases due to an elevated dark rate in the central region of the detector. Recommendations are made regarding observation planning and data analysis.*

Introduction

Over the last decade, little work has been done on calibration for the Advanced Camera for Surveys (ACS) Solar Blind Channel (SBC). This report is the third in a series (Avila et al., 2016; Avila and Chiaberge, 2016) where various aspects of the SBC calibration will be inspected and updated if necessary.

A full investigation of the SBC dark rates was last undertaken in April 2009 (Cox). Since then, the ACS instrument team has continued to include programs designed to monitor the dark rates in its calibration plan. Thanks to this effort, there is now enough data to study any trends or changes in the dark rates and make recommendations to observers.

Data

The Mikulski Archive for Space Telescopes (MAST) contains SBC dark images obtained from a variety of programs. The darks used here are from programs where darks were taken continuously for at least five hours, immediately after the instrument was turned on to conduct observations. This setup allows tracking of how the temperature affects the dark rate. A total of 13 visits from 11 programs meet this criterion (see Table 1).

Proposal ID	**Observation date**	**Exposures**	**Notes**
9022	2002-05-31	30×1200s	
11049	2006-12-12	20×1000s	
11885	2008-12-22	20×1000s	Visit 01
11373	2009-05-31	20×1000s	
11885	2009-08-23	20×1000s	Visit 02
11885	2010-03-22	20×1000s	Visit 03
12391	2011-03-13	20×1000s	
12736	2012-03-12	20×1000s	
13161	2013-03-03	20×1000s	
13598	2014-03-01	20×1000s	
13961	2015-03-03	20×1000s	
14404	2016-03-01	20×1000s	
14513	2017-03-01	20×1000s	

Table 1: List of programs used for this study. Most programs only had one epoch. Program 11885 contained multiple epochs taken at different times, as noted by the column on the right.

Image processing

Images were downloaded from MAST in RAW and FLT format. Dark rates are estimated by taking the mean of all pixels in each RAW image, and then normalizing by the exposure time. Certain pixels are excluded from the calculation; those where the DQ bit in the FLT is non-zero, and the two rows and columns at the edges of the image. The SBC does not have a temperature sensor on the detector, but the temperature is measured on the instrument's enclosure tube. This temperature is recorded at the beginning and end of each exposure and is reported in the MDECODT1 and MDECODT2 header keywords. We use the average temperature of these two as the temperature measurement.

Results

The top panel in Figure 1 shows the dark rate vs temperature for all the datasets. The majority of data sets show a steady dark rate until the temperature reaches $\sim$ 25.5°C. Cox (2009) previously showed that the observations taken in December 2008 (light orange-dashed line) were executed while the observatory was close to the South Atlantic Anomaly

(SAA), and therefore an abnormal peak in the dark rate is observed. Observations from December 2006 (light blue-dashed line) show a similar dark rate vs temperature profile as that problematic set, and indeed Figure 2 shows that those observations also occurred during a close SAA passage.

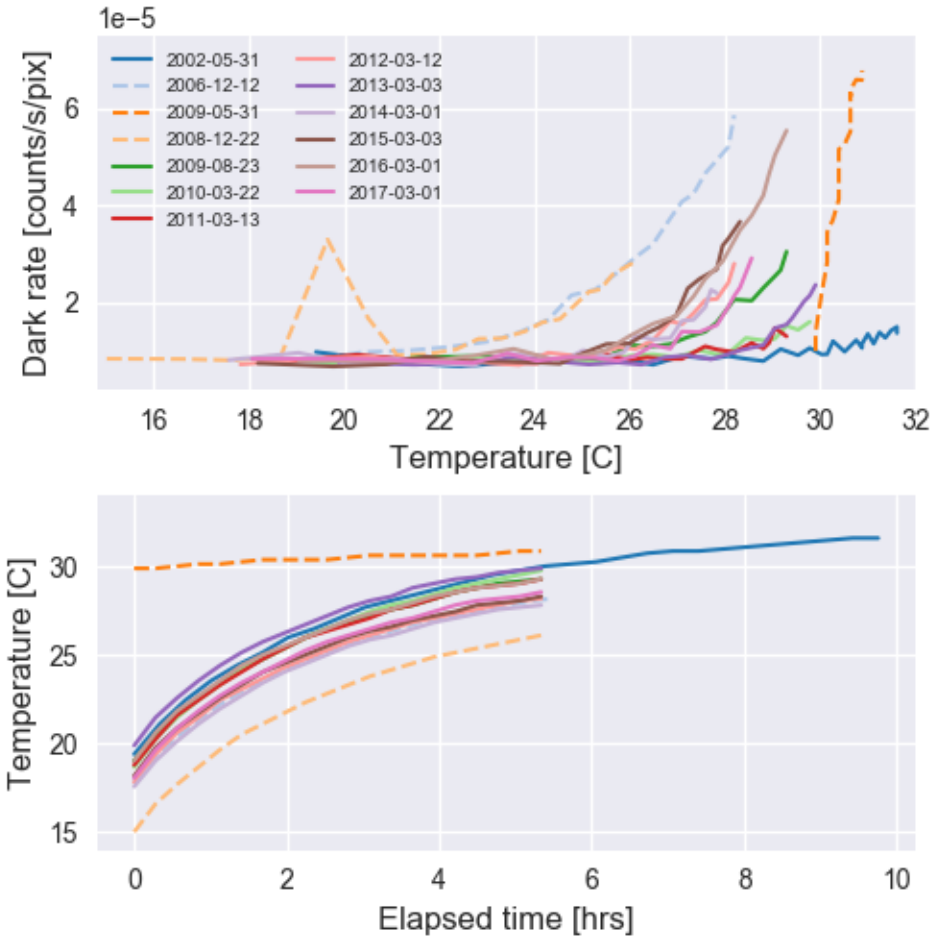

Figure 1: Top panel shows the dark rates vs. temperature measured from all dark rate monitoring programs. The bottom panel shows how the temperature changed from the time the instrument was turned on until the end of the observations. Dashed lines correspond to observations that were excluded from further analysis, see text for details.

The bottom panel in Figure 1 shows how the temperature changes throughout each of the observations. For the most part, the temperature rises with a slowly decreasing rate of change. The shape of most of the curves is the same, with a different initial temperature of the instrument. The one exception to all this is the dataset from May 2009 (dark orange-dashed line), which had an elevated temperature at the beginning of the observations. The SBC had been used for an extended period of time approximately 17 hours before this set of observations. It is possible that the instrument didn't cool down in the intervening time.

Figure 2: Path of HST during the first visit of program 11049, with crosses spaced one minute apart. The red contour shows the extent of the SAA. When these observations occurred, the exclusion region used for SAA passages was smaller.

The two sets of observations taken during the SAA passage and the set that began with an elevated temperature are excluded from further analysis.

Discussion

Figure 1 shows that the dark rate remains stable at low temperatures. The mean dark rate when the instrument is below 25°C is 8.11×10^{-6} cts/pix/s. This is about 35% lower than what is currently reported in Table 3.1 of the ACS Instrument Handbook (Avila, 2017). At this low rate, less than 1% of pixels will have 1 count in a 1000s exposure and a few will have 2 or more counts. At higher temperatures the dark rate begins increasing, and has reached a rate as high as 5.55×10^{-5} cts/pix/s.

It is of interest whether the dark rate has increased in any way during the lifetime of the instrument. We investigate this by plotting the mean dark rate of the last image taken during each of the programs against the observation date (Fig 3). This is the measurement of the dark rate after the instrument has been on for 5 hours. For the 2002 observations

we used the measurement of the dark rate after 5 hours, instead of the last image which corresponds to 10 hours, in order to match the rest of the data. It does appear that the overall final dark rate has been increasing at a rate of 2.0×10^{-6} cts/pix/s/yr. This effect should be monitored on a regular basis from now on.

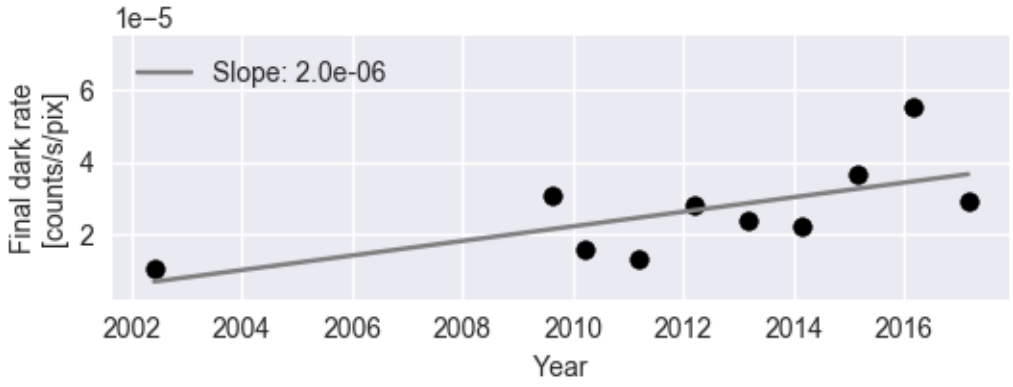

Figure 3: Rate of change of the final dark rate measurement of each visit.

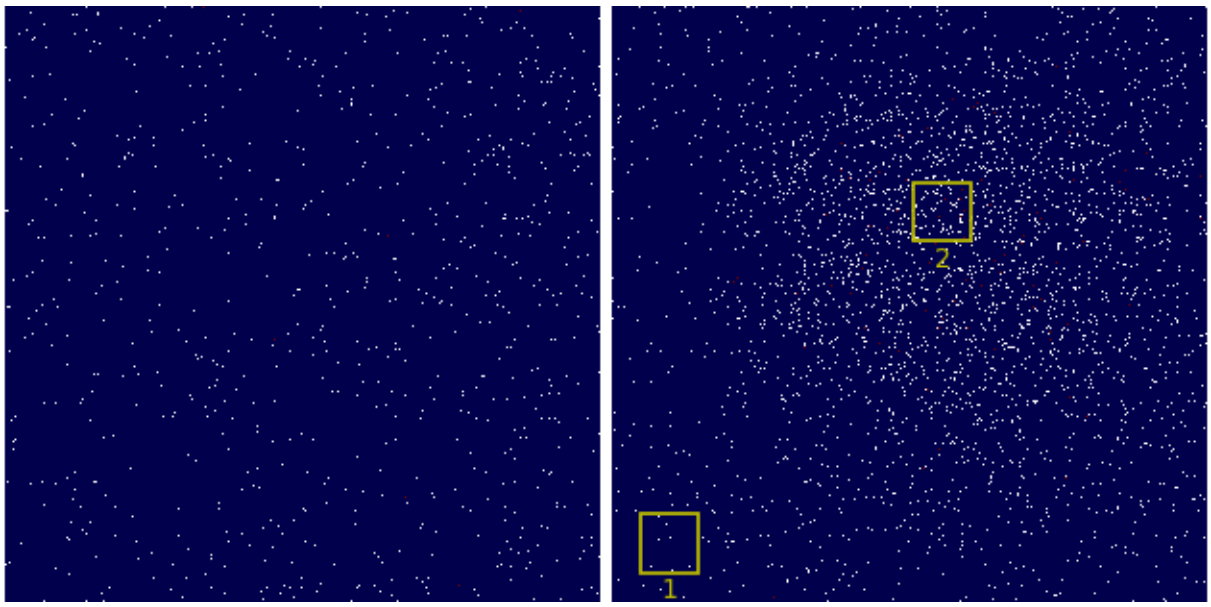

Figure 4: The first (left) and last (right) images from the latest dark monitoring calibration program (PID-14513). The yellow boxes are 100×100 pixels in size, centered around (100,100) and (570,620).

It has been noted that the central region of the detector shows an elevated dark rate at warmer temperatures (Cox, 2004, 2009). Figure 4 shows the first and last images taken in the latest data from March 2017. The central region of the detector does indeed show a concentration of events. This pattern shows up in all the data sets included in this study. To explore this issue further, we examined the dark rates inside two regions on the detector, the two boxes shown in Figure 4. Box 1 is located in the lower left of the detector, where the dark rates are low. Box 2 is located close to the center of the region with the elevated dark

rate. Box 2 avoids the region of the repeller wire (column 500) and the five dead rows on the detector. The ratio of the dark rates measured in these regions is plotted as a function of temperature in Figure 5. The ratio of the dark rate in the two regions doubles at T$\sim$ 25°C and rapidly grows at greater temperatures. The region in Box 1 maintains a steady dark rate even at elevated temperatures. This indicates that the increase in the overall dark rate is driven by the elevated dark rate of the central region of the detector. Given this information, the ACS instrument team should explore the possibility of defining a new aperture position centered close to Box 1, assuming that flat fields in those regions are stable enough for such a setup. This aperture could be used for observations of compact sources where it is not necessary to have the full aperture of the detector.

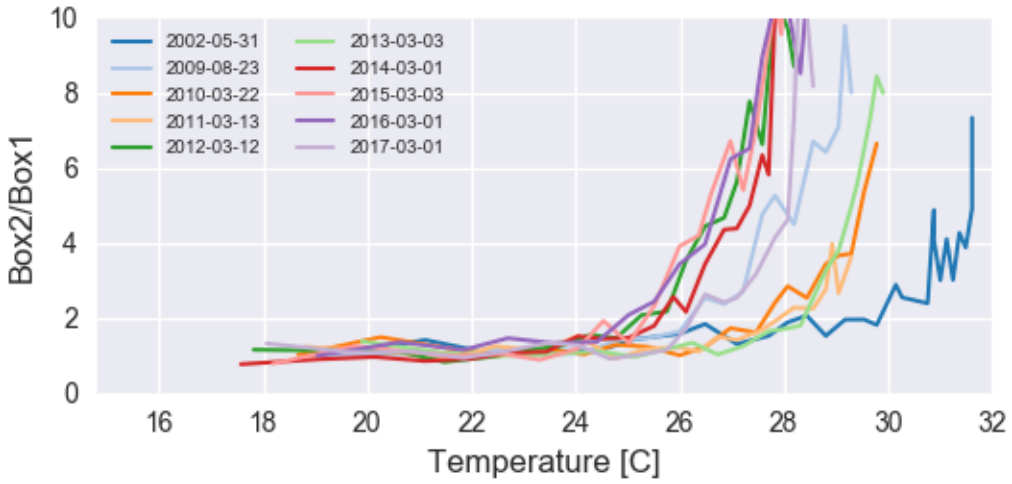

Figure 5: Ratio of dark rates in two different regions in the detector as a function of temperature.

Conclusion

The dark rate for the SBC remains as stable as ever. It remains steady while the instrument is $\lesssim$ 25.°C. Above that temperature, the central region of the detector begins to experience an increasingly higher dark rate. That being the case, dark frames cannot be subtracted from science observations like they are with CCDs. Unlike CCDs, MAMA dark images are not meant to capture hot and warm pixels. Instead, dark rate in MAMA detectors shows up as random background noise. It is therefore not necessary for the pipeline to change its current mode of operation for SBC images, which is to omit dark subtraction.

For the purposes of scientific analysis, the dark rate can be subtracted along with the background noise, at least when the detector is still $\lesssim$ 25.°C. Above that temperature, users should still be able to do a local subtraction, but should be aware of the pattern present in the dark rate.

Contact scientists should ensure, during Phase II reviews, that SBC visits are of an appropriate length so that the instrument remains at a temperature $\lesssim$ 25.°C.

No delivery of dark frames to the calibration pipeline should be necessary, but the instrument team should keep the monitoring program in its calibration plans for the lifetime of the instrument.

Assuming there are no flat fielding or other issues, the ACS instrument team should explore the possibility of defining a new aperture position close to the lower left of the detector where the dark rate remains steady even at elevated temperatures.

Acknowledgements

The author would like to thank Gabe Brammer and Joanna Taylor for their help with plotting the telescope's orbital position during an observation. Many thanks to the following ACS team members who provided feedback to improve this report: Andrea Bellini, Ralph Bohlin, David Borncamp, Marco Chiaberge, Samantha Hoffmann, and Jenna Ryon.

This work made use of the following software packages: `ipython` (Pérez and Granger, 2007), `numpy` and `scipy` (van der Walt et al., 2011), `matplotlib` (Hunter, 2007), and `astropy` (Bradley et al., 2016).

References

R. J. Avila. *Advanced Camera for Surveys Instrument Handbook for Cycle 25 v. 16.0*. January 2017.

R. J. Avila and M. Chiaberge. Photometric Aperture Corrections for the ACS/SBC. Technical Report ISR ACS 2016-05, Space Telescope Science Institute, September 2016.

R. J. Avila, M. Chiaberge, and R. Bohlin. SBC Internal Lamp P-flat Monitoring. Technical Report ISR ACS 2016-02, Space Telescope Science Institute, March 2016.

Larry Bradley, Brigitta Sipocz, Thomas Robitaille, Erik Tollerud, Christoph Deil, Zè Vinícius, Kyle Barbary, Hans Moritz Günther, Azalee Bostroem, Michael Droettboom, Erik Bray, Lars Andersen Bratholm, T. E. Pickering, Matt Craig, Sergio Pascual, Johnny Greco, Axel Donath, Wolfgang Kerzendorf, StuartLittlefair, Geert Barentsen, Francesco D'Eugenio, and Benjamin Alan Weaver. astropy/photutils v0.2.2, September 2016. URL `https://doi.org/10.5281/zenodo.155353`.

C. Cox. SBC Dark and Cumulative Images. Technical Report ISR ACS 2004-14, Space Telescope Science Institute, July 2004.

C. Cox. Re-measurement of ACS/SBC dark images. Technical Report ISR ACS 2009-02, Space Telescope Science Institute, April 2009.

J. D. Hunter. Matplotlib: A 2d graphics environment. *Computing In Science & Engineering*, 9(3):90–95, 2007.

Fernando Pérez and Brian E. Granger. IPython: a system for interactive scientific computing. *Computing in Science and Engineering*, 9(3):21–29, May 2007. ISSN 1521-9615. doi: 10.1109/MCSE.2007.53. URL `http://ipython.org`.

Stéfan van der Walt, S. Chris Colbert, and Gaël Varoquaux. The numpy array: a structure for efficient numerical computation. *CoRR*, abs/1102.1523, 2011. URL `http://arxiv.org/abs/1102.1523`.